

Fatigue strength assessment of heavy section ductile irons through the average strain density energy criterion

Paolo Ferro¹  | Thomas Borsato¹ | Filippo Berto²  | Carlo Carollo³

¹Department of Engineering and Management, University of Padova, Vicenza, Italy

²Department of Engineering Design and Materials, NTNU, Trondheim, Norway

³VDP Fonderia SpA, Schio, Italy

Correspondence

Paolo Ferro, Department of Engineering and Management, University of Padova, Stradella San Nicola 3, 36100 Vicenza, Italy.

Email: paolo.ferro@unipd.it

Abstract

In recent years, strain energy-based criteria used to predict the static and fatigue strength of notched components have attracted the attention of many researchers. The reasons are a lot. The energy density is first of all a scalar quantity, and when calculated by finite element methods, it does not need a fine mesh, which speeds up significantly the design of complex as well as large structures. Among these approaches, the average strain energy density (ASED) states that failure will occur when the strain energy averaged over a control volume of radius R_c will reach a critical value. R_c is a material property to be determined by experiments. In the present work, the ASED criterion is applied to heavy section ductile irons containing defects. It is found that a narrow ASED-based scatter band is able to summarize the fatigue behaviors of different ductile irons families.

KEYWORDS

cast iron, defects, fatigue, microstructure, strain energy density

1 | INTRODUCTION

In literature, many approaches were developed to assess the fatigue behavior of notched and/or cracked components. Nominal stress,¹ structural stress,¹ and local methods^{1,2} are some of them. By focusing on local approaches, perhaps, the notch stress intensity factor (N-SIF)-based criterion³ is the most famous. The well-known concept of stress intensity factors (SIFs) describing the stress singularity at crack tips or slit tips under linear-elastic material conditions is transferred to pointed reentrant corner notches (e.g., V-notches, stepped bars, and weld toe notches). The SIF concept has been substantially extended since Williams⁴ basic contribution on stress fields at angular corners. Williams' solution has been widely used under the name "eigenfunction expansion method". It should be noted that the elastic N-SIFs are used to describe the fatigue strength of fillet-welded attachment joints as well as the fracture toughness of brittle materials. Even if this method is widely used in literature, the major disadvantage is that it does not allow comparing fatigue behavior of parts characterized by different V notch opening angles. This is due to the value of the exponent in the definition of the NSIF, which is a function of the notch opening angle.

In order to overcome this problem, the static and fatigue strength of sharp V-notched components can be assessed by means of energetic approaches, such as the J-integral or the strain energy density (SED) averaged over a control volume.⁵⁻⁷ The idea of considering a quantity averaged over a control volume instead of a maximum stress or strain goes back to Neuber^{8,9} who formulated the hypothesis of an "elementary material volume" or "microstructural support length" for this purpose. On this track, and following the idea of Beltrami,¹⁰ the local SED approach has been proposed and analytically developed by Lazzarin and Zambardi.⁵ In the case of sharp notch tips, not only the stresses at the notch tip tend towards infinity but also the SED. Contrary to this, the averaged SED in a local finite volume around the notch

(or crack) tip has a finite value. This value is considered to be the material parameter that describes the initiation of brittle fracture or fatigue failure. The control volume around the notch tip is characterized by a critical radius, R_c , that is a material property, as well. The critical radius was found to be equal to 0.28 and 0.12 mm in the case of steel and Al-alloy welded joints, respectively. Unfortunately, the characterization of such parameter for a given material is not simple because several fatigue tests on smooth and notched components are required. In Berto et al,¹¹ the SED approach has been applied to a traditional ferritic ductile cast iron under multiaxial fatigue loading.

The present work is aimed at applying the ASED criterion to the fatigue strength assessment of three kinds of heavy section ductile irons containing killer-named defects such as shrinkage porosities or degenerated graphite particles induced by long solidification times. As a matter of fact, such kind of defects act like stress concentrator factors in a similar way like notches or cracks in a homogeneous material. An ASED value can thus be calculated at killer-defect's tip, which is supposed to quantify the fatigue strength of the cast irons under investigation.

2 | MATERIALS AND METHODS

The materials considered in the present work are heavy section castings made out of two traditional ductile irons (GJS 400-18 LT and GJS 700-2) and a new generation solution strengthened ferritic ductile iron^{12,13} (named solution strengthened ferritic ductile iron [SSF-DI]).

Specimens were taken from heavy section castings characterized by solidification times of about 2.5 h (Figure 1). Their mechanical properties were reported in Table 1.

Shape and dimensions of graphite particles have been evaluated according to ASTM E2567 and ASTM A247 standards. Minimum shape factor (SF) (Equation 1) value to qualify a particle as a nodule was assumed 0.5. The total number of nodules was divided by the total area of observation (about 1000 mm²) in order to calculate the nodule count (mm⁻²).

$$SF = \frac{Area_{Graphite\ particle}}{\pi \left(\frac{Max\ Feret\ diameter^2}{4} \right)} \quad (1)$$

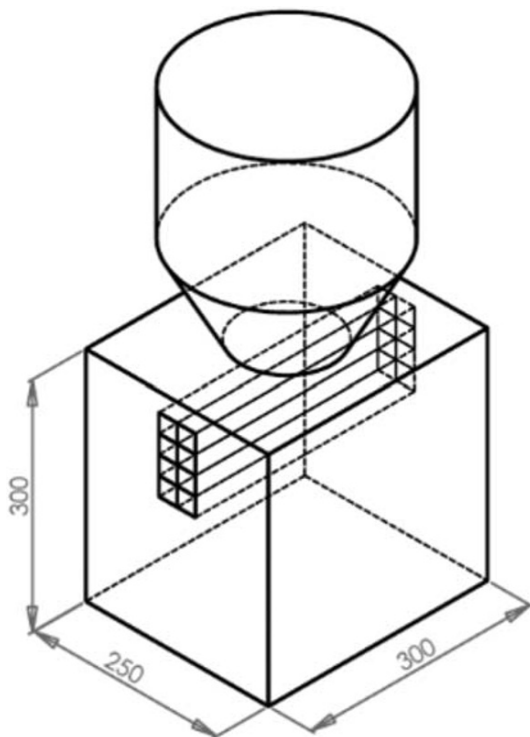


FIGURE 1 Heavy section casting and zones where samples were cut from (solidification times ~2.5 h)

TABLE 1 Static mechanical properties of the analyzed cast irons

Cast iron grade	Casting	UTS (MPa)	Yield stress (MPa)	Elongation at fracture (%)
GJS 700-2	I	579	364	2.6
	II	513	368	1.9
	III	511	410	2
GJS 400-18 LT	IV	383	250	19.9
SSF-DI	V	485	381	18

Note: specimens taken from the longest to solidify zones shown in Figure 1.

Abbreviations: SSF-DI, solution strengthened ferritic ductile iron; UTS, ultimate tensile strengths.

In Equation 1, the Feret diameter is the distance between the two parallel tangential lines restricting the graphite nodule. Uniaxial tension fatigue life tests were carried out at room temperature using a universal MTS machine (250 kN), a load frequency of 15 Hz, and zero load ratio ($R = 0$), like in the works by Borsato et al.^{14,15}

After fatigue tests, fractography has been carried out on the surface of broken specimens using a field emission gun–environmental scanning electron microscope (FEG-ESEM) (FEI, Quanta 250 FEG) in order to identify crack initiation zones and measure their dimensions ($\sqrt{\text{area}}$). It was found that cracks initiated at microstructural defects such as microshrinkage cavities or degenerated graphite particles near the surface of the specimens as shown in Figure 2.

The fatigue data have been analyzed by using the ASED criterion.⁵ According to it, each number of cycles to failure (N) is characterized by a critical value of the SED averaged over a control volume of radius R_c surrounding the stress singularity dominated zone. In particular, in this work, the stress singularity dominated zone is considered to be that surrounding the tip of the “killer” defect modeled as a crack of length equal to the mean value of the dimension ($\sqrt{\text{area}}$) measured on the fracture surfaces for each casting (Figure 3).

Considering N equal to 2×10^6 , the following equation holds true^{2,5}:

$$\Delta W = \frac{\int_A W dA}{\pi R_c^2} = \frac{\Delta \sigma_A^2}{2E} = \Delta W_c \quad (2)$$

where W is the SED, $\Delta \sigma_A$ is the stress range at 2×10^6 cycles of the ideal defects-free material, and E is the Young's modulus. R_c is the critical radius supposed to be a material property only.

The fatigue limit, in the case of material without microshrinkages porosities or degenerated graphite particles ($\Delta \sigma_A$ in Equation 2), has been estimated by means of Murakami's equation¹⁶:

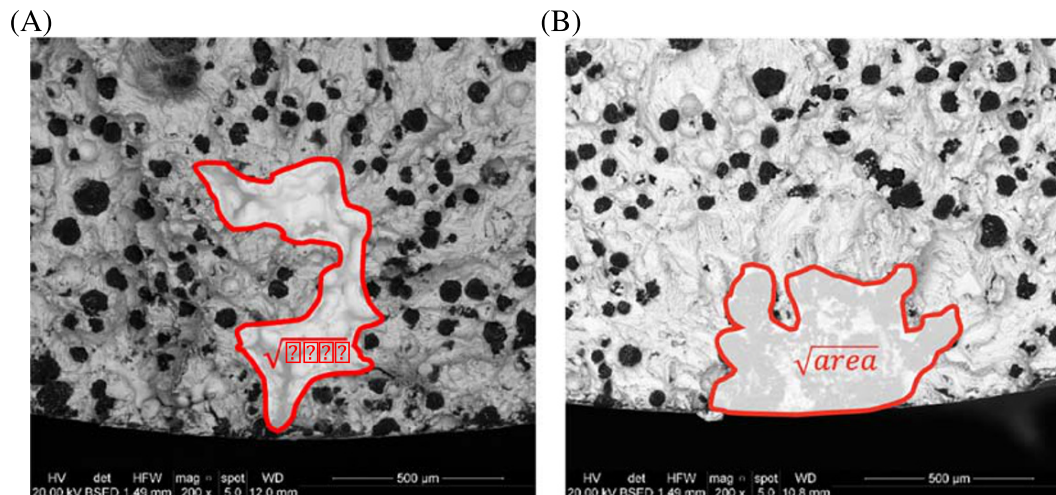


FIGURE 2 “Killer”-defects detected in fracture surfaces: (A) shrinkage porosity and (B) degenerate graphite

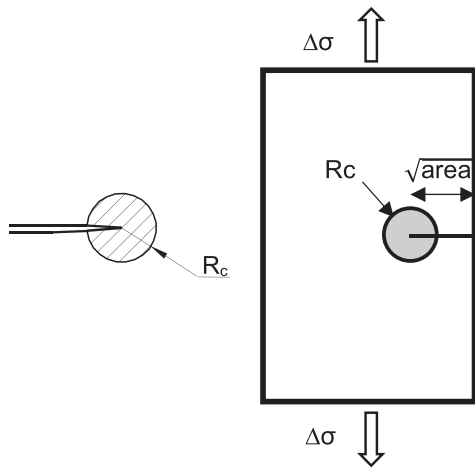


FIGURE 3 Specimens were modeled with a lateral crack of length equal to the killer defect dimension ($\sqrt{\text{area}}$); the control volume surrounding the crack tip is also shown

$$\sigma_{est} = F_{loc} \frac{(HV + 120)}{\sqrt{\text{area}}^{1/6}} \left(\frac{1-R}{2} \right)^\alpha, \quad (3)$$

where $\sigma_{est} = \Delta\sigma_A/2$, F_{loc} is the location factor equal to 1.41; HV is the Vickers hardness; α is a material dependent coefficient that for ductile irons is given by $0.371 + HV \times 10^{-417}$; and R is the load ratio. The $\sqrt{\text{area}}$ value has been chosen to be equal to the mean graphite nodule diameter (considered as intrinsic material defect¹⁸) for each casting analyzed (Table 2). As a matter of fact, the low strength of graphite nodule makes it mechanically equivalent to a defect or a hole.¹⁹ Therefore, Equation 3 can be written as

$$\sigma_{est} = F_{loc} \frac{(HV + 120)}{\sqrt{\text{nodule diameter}}^{1/6}} \left(\frac{1-R}{2} \right)^\alpha. \quad (4)$$

Now, the critical ASED value at 2 million cycles is calculated by means of Equation 5^{2,5}:

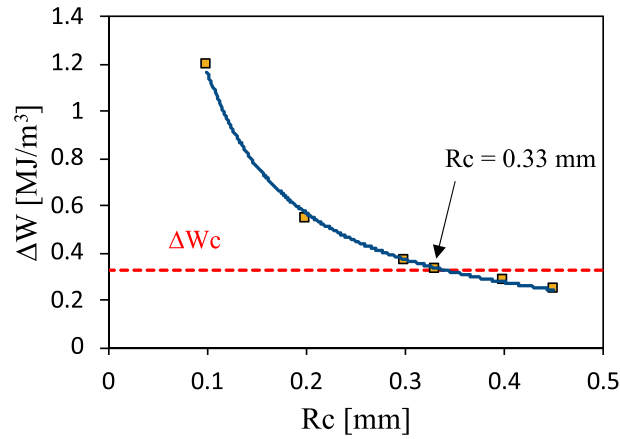
$$\Delta W_C \approx \frac{(\Delta\sigma_A)^2}{2E}, \quad (5)$$

with $\Delta\sigma_A = 2 \cdot \sigma_{est}$. Values of the mean $\sqrt{\text{area}}$, mean graphite nodule diameter, and critical SED ΔW_C for each casting analyzed are collected in Table 2.

TABLE 2 Values of mean $\sqrt{\text{area}}$, mean graphite nodule diameter, nodule count, and critical strain energy density (SED) ΔW_C for each casting analyzed

Castings	Mean $\sqrt{\text{area}}$ microshrinkage porosities (μm)	Mean graphite nodule diameter (μm)	Nodule count (mm^{-2})	ΔW_C (MJ/m^3)
GJS 700-2	720	66	26	0.0357
GJS 700-2	435	45	52	0.405
GJS 700-2	513	55	46	0.379
SSF-DI	624	49	31	0.350
GJS 400-18	646	60	38	0.218

Note: The three kinds of GJS 700-2 differ in inoculant chemical composition used for their production.²⁰
Abbreviation: SSF-DI, solution strengthened ferritic ductile iron.

FIGURE 4 Numerical calculation of R_c 

To evaluate the value of R_c , plane strain finite element simulations have been performed using the geometry schematized in Figure 3. By varying the value of R_c , the plot ΔW versus R_c was first obtained (Figure 4). Finally, the point where $\Delta W = \Delta W_c$ was determined (Figure 4).

The R_c value equal to 0.33 mm was calculated for all castings, which is the same result obtained by Berto et al.¹¹

3 | RESULTS AND DISCUSSION

When dealing with heavy section ductile iron castings characterized by long solidification times as well as low cooling rates, the major defects that negatively affect the resistance of the material are correlated to degenerated forms of

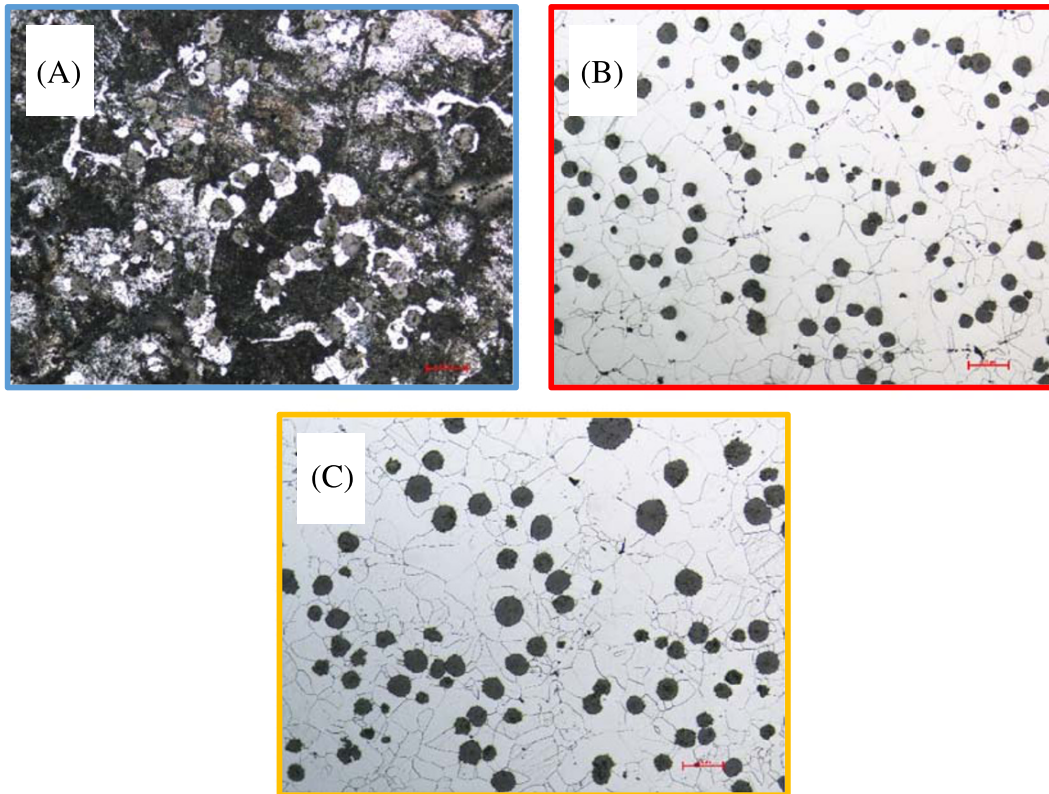


FIGURE 5 Micrographs showing the microstructure of the analyzed cast irons: (A) GJS 700-2; (B) GJS 400-18 LT; and (C) solution strengthened ferritic ductile iron (SSF-DI)

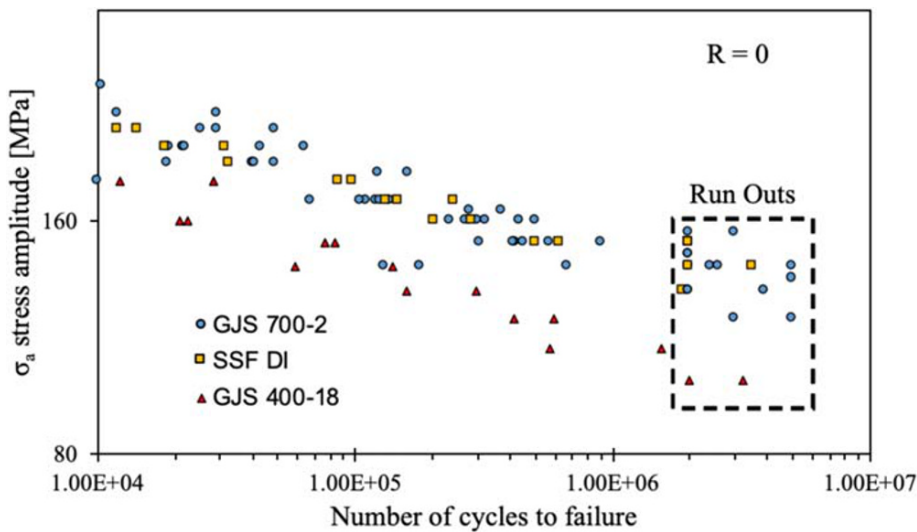


FIGURE 6 Fatigue test results

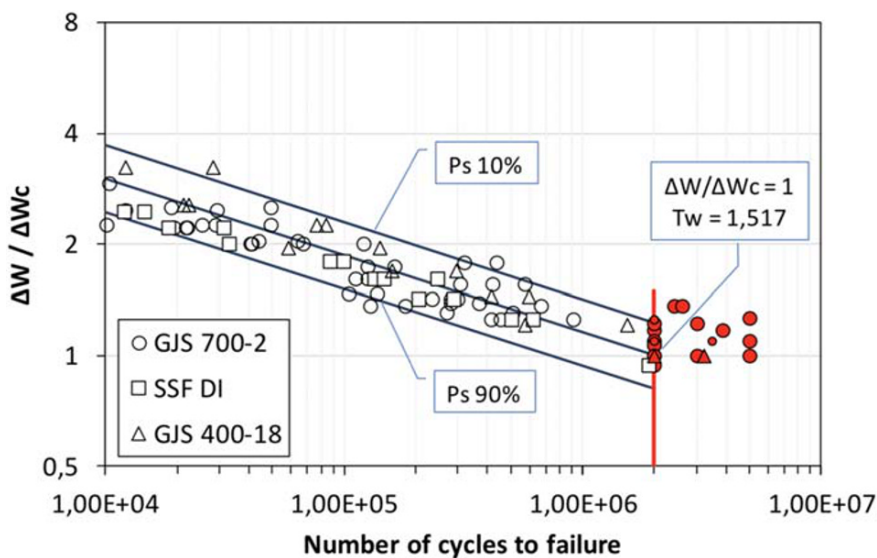


FIGURE 7 Synthesis in terms of ratio between the effective and the critical strain energy density (SED) for all data from different ductile irons containing defects considering $R_c = 0.33$ mm. T_w is the scatter index referring to $P_s = 10\%$ and $P_s = 90\%$. P_s stands for survival probability, whereas red symbols stand for “run out”. SSF, solution strengthened ferritic

graphite particles, low nodule count, microshrinkage porosities, and inclusions. From Table 1, it is observed that because of the long solidification time and defects induced by it in the alloy, the ultimate tensile strengths (UTS) of the GJS 700-2 and GJS 400-18 LT do not reach the required standards (700 and 400 MPa, respectively). Moreover, it is worth observing that the SSF-DI shows much higher mechanical properties compared with the GJS 400-18 LT while keeping almost the same value of the elongation at fracture. Figure 5 shows the micrograph of the three kinds of alloys analyzed.

Results of fatigue tests in terms of stress amplitude are reported in Figure 6.

Using the value of $R_c = 0.33$ mm, the average SED (ΔW) was calculated for all specimens by applying the experimental fatigue strength to the model containing a crack with length equal to the size of the corresponding killer defect.

It can be observed that, when considering the ratio between the effective (ΔW) and the critical SED (ΔW_c), all the fatigue data (traditional and solution strengthened ferritic ductile irons) fall into a narrow scatter band, with a scatter index $T_w = 1.517$ (Figure 7).

4 | CONCLUSIONS

The fatigue strength of defects containing specimens, made out of traditional (GJS 400-18 and GJS 700-2) as well as new generation solution strengthened ferritic ductile irons, has been compared using the SED criterion. The synthesis

allows obtaining a narrow SED-based scatter band with a scatter index equal to 1.517 when considering all data and the critical radius $R_c = 0.33$ mm.

ACKNOWLEDGEMENTS

The authors would like to thank VDP Fonderia SpA for the material supply, financial, and technical support to the project.

CONFLICT OF INTEREST

The authors declare no conflict of interest.

ORCID

Paolo Ferro  <https://orcid.org/0000-0001-8682-3486>

Filippo Berto  <https://orcid.org/0000-0001-9676-9970>

REFERENCES

1. Fuštar B, Lukačević I, Dujmović D. Review of fatigue assessment methods for welded steel structures. *Adv Civil Eng*. 2018;1-16. <https://doi.org/10.1155/2018/3597356>
2. Livieri P, Lazzarin P. Fatigue strength of steel and aluminium welded joints based on generalised stress intensity factors and local strain energy values. *Int J Fract*. 2005;133:247-276.
3. Lazzarin P, Tovo R. A notch stress intensity factor approach to the stress analysis of welds. *Fatigue Fract Engng Mater Struct*. 1998;21(9):1089-1103.
4. Williams ML. Stress singularities resulting from various boundary conditions in angular corners of plates in tension. *J Appl Mech*. 1952;19(1952):526-528.
5. Lazzarin P, Zambardi R. A finite-volume-energy based approach to predict the static and fatigue behaviour of components with sharp V-shaped notches. *Int J Fract*. 2001;112:275-298.
6. Lazzarin P, Berto F. Control volumes and strain energy density under small and large scale yielding due to tension and torsion loading. *Fatigue Fract Engng Mater Struct*. 2008;31:95-107.
7. Lazzarin P, Berto F. Some expressions for the strain energy in a finite volume surrounding the root of blunt V-notches. *Int J Fract*. 2005;135:161-185.
8. Neuber H. *Kerbspannungslehre*. 2nd ed. Berlin: Springer-Verlag; 1958.
9. Neuber H. *Kerbspannungslehre*. 3rd ed. Berlin: Springer-Verlag; 1985.
10. Beltrami E. Sulle condizioni di resistenza dei corpi elastici. In: *Il Nuovo Cimento 18 (in Italian)*; 1885.
11. Berto F, Lazzarin P, Tovo R. Multiaxial fatigue strength of severely notched cast iron specimens. *Int J Fatigue*. 2014;67:15-27.
12. UNI EN 1563. : 2012, Founding—spheroidal graphite cast irons.
13. Larker R. Solution strengthened ferritic ductile iron ISO 1083/JS/500-10 provides superior consistent properties in hydraulic rotators. *Overseas Foundry*. 2009;6:343-351.
14. Borsato T, Ferro P, Berto F, Carollo C. Mechanical and fatigue properties of heavy section solution strengthened ferritic ductile iron castings. *Adv Eng Mat*. 2016;18:2070-2075.
15. Borsato T, Ferro P, Berto F, Carollo C. Fatigue strength improvement of heavy-section pearlitic ductile iron castings by in-mould inoculation treatment. *Int J Fatigue*. 2017;102:221-227.
16. Murakami Y. *Metal Fatigue: Effects of Small Defects and Nonmetallic Inclusions*. Elsevier; 2002 ISBN: 0080440649.
17. Endo M, Iseda K. Prediction of the fatigue strength of nodular cast irons under combined loadings. *Int J Mod Phys B*. 2006;20:3817-3823.
18. Endo M. Effects of graphite shape, size and distribution on the fatigue strength of spheroidal graphite cast irons. *J Soc Mater Sci Japan*. 1989;38:1139-1144. <https://doi.org/10.2472/jsms.38.1139>
19. Nisitani H, Murakami Y. Part of spheroidal graphite of nodular iron casting under bending or torsional fatigue. *Res Mach*. 1973;25(4):543-546.
20. Borsato T, Ferro P, Berto F, Carollo C. Mechanical and fatigue properties of pearlitic ductile iron castings characterized by long solidification times. *Eng Fail Anal*. 2017;79:902-912.

How to cite this article: Ferro P, Borsato T, Berto F, Carollo C. Fatigue strength assessment of heavy section ductile irons through the average strain density energy criterion. *Mat Design Process Comm*. 2020;1-7. <https://doi.org/10.1002/mdp2.197>